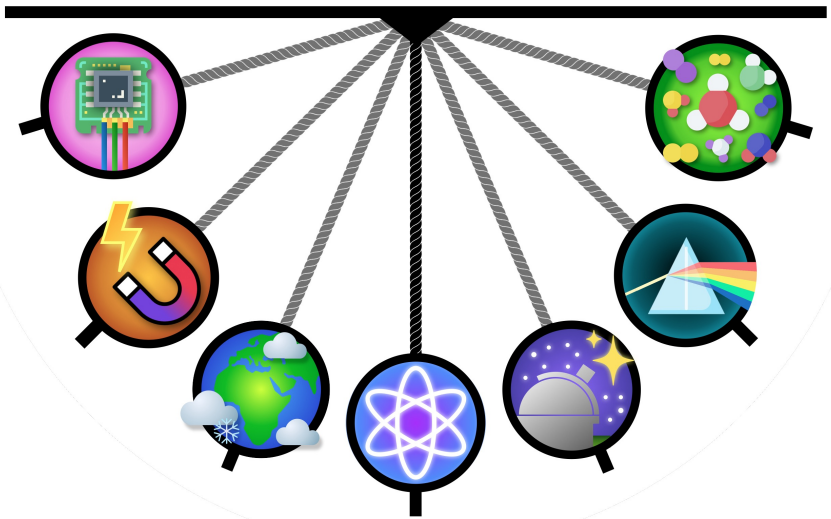
PhDay FÍSICAS 2025

FACULTAD DE CIENCIAS FÍSICAS

ESCUELA DE DOCTORADO
UNIVERSIDAD COMPLUTENSE DE MADRID

2025 PhDay Físicas



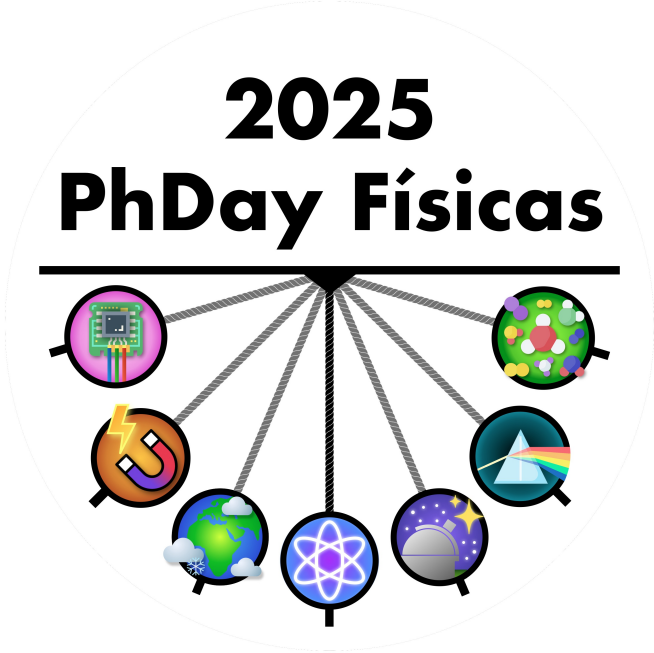
Premios patrocinados por EXINA S.L.

La Casa del Estudiante
UNIVERSIDAD COMPLUTENSE DE MADRID

PhDay FÍSICAS 2025

FACULTAD DE CIENCIAS FÍSICAS

ESCUELA DE DOCTORADO
UNIVERSIDAD COMPLUTENSE DE MADRID



3 y 4 noviembre 2025: en Gabinete de Físicas
exposición de pósteres
(de 11h a 13h y de 15h30m a 17h30m)
presentación 1 min pósteres
(a las 12h:30m el 3 de nov y a las 16h:30m el 4 nov)

7 noviembre 2025: en Sala de Grados
exposición oral de los finalistas (10h)
y entrega de premios (13h30m)

La Casa del Estudiante
UNIVERSIDAD COMPLUTENSE DE MADRID

Premios patrocinados por EXINA S.L.

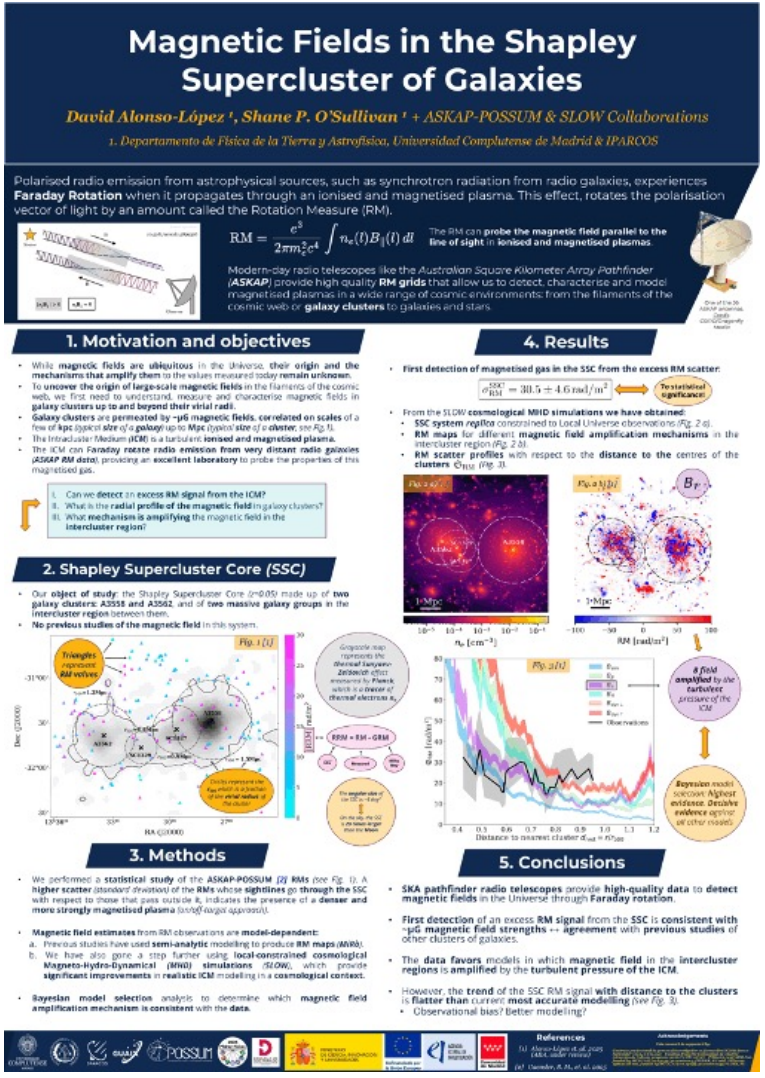
2025 PhDay Físicas

Lista de participantes PhDay Físicas 2025

ESCUELA DE DOCTORADO
UNIVERSIDAD COMPLUTENSE DE MADRID

n°	Nombre y apellidos	Dpto.	Director(es) de tesis	Programa de doctorado
1	David Alonso López	FTA	Shane P. O'Sullivan y Armando Gil de Paz	Astrofísica
2	Daniel De Maeseneire Martínez	FTA	Blanca Ayarzagüena y Natalia Calvo	Física
3	Sebastián Duarte Cano	EMFTEL	Rodrigo Garcia Hernansanz	Física
4	Lucía Escudero Palencia	FTA	Maurizio Mattesini y Aldo Zollo	Física
5	Jorge Estrada Álvarez	FM	Elena Díaz García, Francisco Domínguez-Adame Acosta	Física
6	Tahimy Fuentes Alvarez	FTA	Carlos Ordóñez	Física
7	Rafael Fuster Rico	FM	Javier Tornos Castillo y Jacobo Santamaría Sánchez-Barriga	Física
8	Juan José Gálvez Viruet	FT	Felipe J. Llanes Estrada y María Gómez Rocha	Física
9	María Garrido Segovia	FM	Elena Navarro Palma, José Miguel García Martín y Ana Espinosa de los Monteros Royo	Física
10	Gonzalo Gómez Muñoz	FM	Belén Sotillo Buzarra y F. Javier Solís Céspedes	Física
11	Lucía Gutiérrez González	FTA	María Luisa Montoya Redondo	Física
12	Paula Macías Pardo	FTA	Armando Gil de Paz, Cristina Catalán Torrecilla	Astrofísica
13	Amanda Nathali Nerio Aguirre	EMFTEL	José Antonio Briz Monago y María José García Borge	Física
14	Sergio Pérez Montero	FTA	Jorge Álvarez Solas	Física
15	Carlota Prieto Jiménez	FTA	Javier Álvarez Márquez y Michele Perna	Astrofísica
16	Solange Suli Silicaro	FTA	David Barriopedro Cepero	Física

Departamentos: Física de Materiales (FM), Física Teórica (FT), Física de la Tierra y Astrofísica (FTA), Óptica (O), Estructura de la Materia, Física Térmica y Electrónica (EMFTEL)

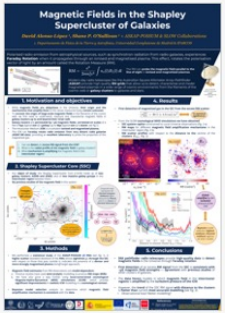


PhDay FÍSICAS 2025

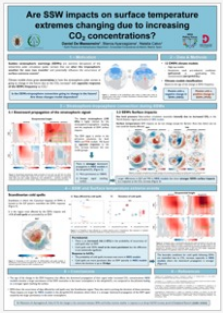
2025 PhDay Físicas

La Casa del Estudiante — Universidad Complutense de Madrid

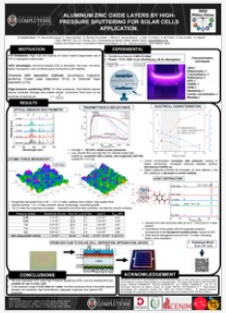
Escuela de Doctorado — Universidad Complutense de Madrid



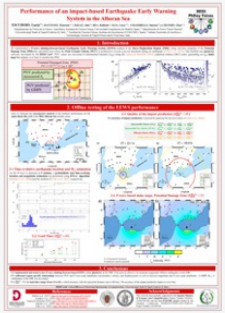
1



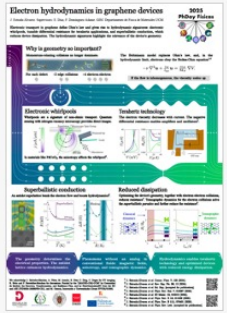
2



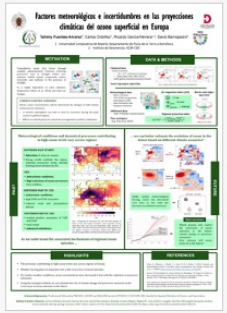
3



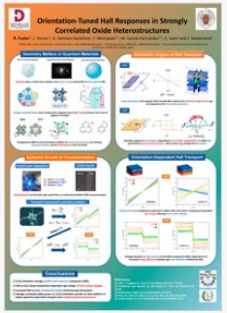
4



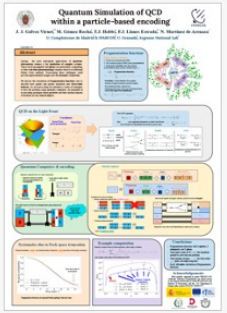
5



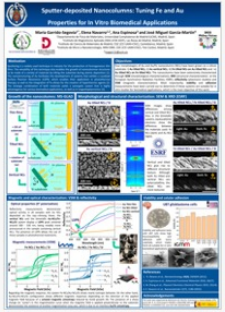
6



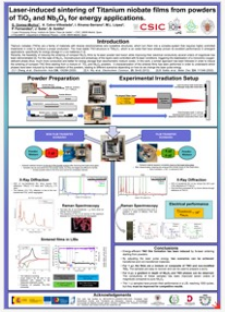
7



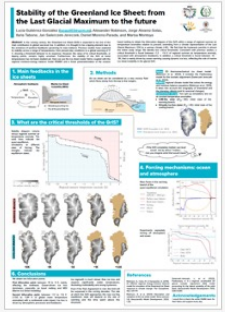
8



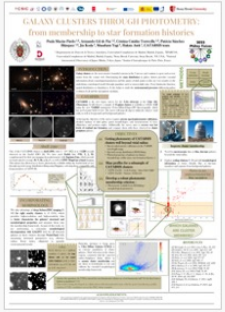
9



10



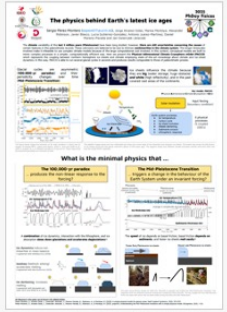
11



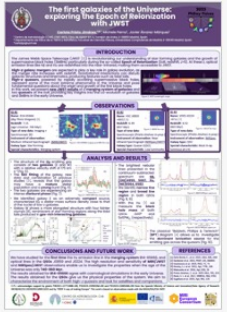
12



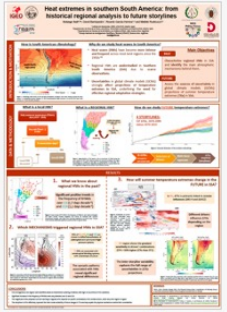
13



14



15



16

PhDay FÍSICAS 2025

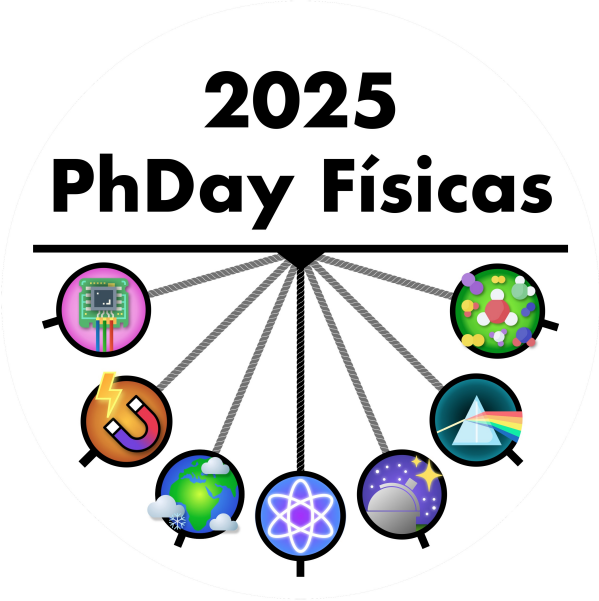
FACULTAD DE CIENCIAS FÍSICAS

ESCUELA DE DOCTORADO
UNIVERSIDAD COMPLUTENSE DE MADRID

3 y 4 noviembre 2025

a las 12h:30m y 16h:30m

Presentaciones de **1 minuto** de los pósteres



La Casa del Estudiante
UNIVERSIDAD COMPLUTENSE DE MADRID

FACULTAD DE CIENCIAS FÍSICAS

1

Magnetic Fields in the Shapley Supercluster of Galaxies

David Alonso López

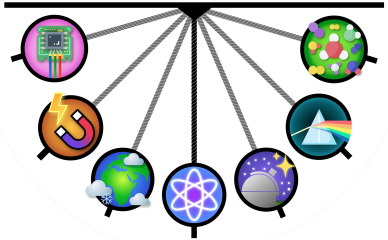
ESCUELA DE DOCTORADO
UNIVERSIDAD COMPLUTENSE DE MADRID



1

Nombre	David
Apellidos	Alonso López
Departamento	FTA
Doctorado	Astrofísica
Director/es de la Tesis	Shane P. O'Sullivan y Armando Gil de Paz
Título de la contribución	***Magnetic Fields in the Shapley Supercluster of Galaxies***

2025
PhDay Físicas

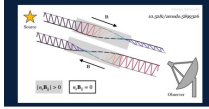


Magnetic Fields in the Shapley Supercluster of Galaxies

David Alonso-López [1], Shane P. O'Sullivan [1] + ASKAP-POSSUM & SLOW Collaborations

1. Departamento de Física de la Tierra y Astrofísica, Universidad Complutense de Madrid & IPARCOS

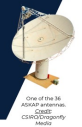
Polarised radio emission from astrophysical sources, such as synchrotron radiation from radio galaxies, experiences **Faraday Rotation** when it propagates through an ionised and magnetised plasma. This effect, rotates the polarisation vector of light by an amount called the Rotation Measure (RM).



$$\mathrm{RM} = \frac{e^3}{2\pi m_e^2 c^4} \int n_e(l) B_\parallel(l)\, dl$$

The RM can **probe the magnetic field parallel to the line of sight** in **ionised and magnetised plasmas**.

Modern-day radio telescopes like the *Australian Square Kilometer Array Pathfinder* (***ASKAP***) provide high quality **RM grids** that allow us to detect, characterise and model magnetised plasmas in a wide range of cosmic environments: from the filaments of the cosmic web or **galaxy clusters** to galaxies and stars.



One of the 36 ASKAP antennas. © CSIRO/Wirrngarrity Media

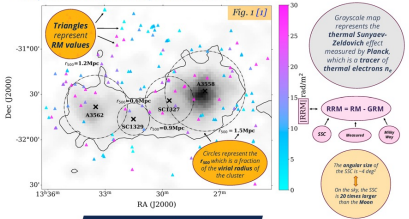
1. Motivation and objectives

- While **magnetic fields are ubiquitous** in the Universe, **their origin and the mechanisms that amplify them** to the values measured today **remain unknown**.
- To **uncover the origin of large-scale magnetic fields** in the filaments of the cosmic web, we first need to understand, measure and characterise magnetic fields in **galaxy clusters up to and beyond their virial radii**.
- **Galaxy clusters** are **permeated by ~μG magnetic fields**, **correlated on scales** of a few of **kpc** *(typical* **size** *of a* ***galaxy****)* up to **Mpc** *(typical* **size** *of a* ***cluster****, see Fig.1)*.
- The Intracluster Medium (***ICM***) is a turbulent **ionised and magnetised plasma.**
- The ICM can **Faraday rotate radio emission from very distant radio galaxies** (***ASKAP RM data***), providing an **excellent laboratory** to probe the properties of this magnetised gas.

I. Can we **detect** an **excess RM signal from the ICM?**
II. What is the **radial profile of the magnetic field** in galaxy clusters?
III. What **mechanism is amplifying** the magnetic field in the **intercluster region**?

2. Shapley Supercluster Core *(SSC)*

- Our **object of study**: the Shapley Supercluster Core *(z=0.05)* made up of **two galaxy clusters: A3558 and A3562**, and of **two massive galaxy groups** in the **intercluster region** between them.
- **No previous studies of the magnetic field** in this system.



3. Methods

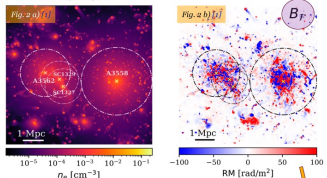
- We performed a **statistical study** of the **ASKAP-POSSUM** ***[2]*** **RMs** *(see Fig. 1)*. A **higher scatter** *(standard deviation)* of the **RMs** whose **sightlines** go **through the SSC** with respect to those that pass outside it, indicates the presence of a **denser and more strongly magnetised plasma** *(on/off-target approach)*.
- **Magnetic field estimates** from RM observations are **model-dependent:**
  a. Previous studies have used **semi-analytic** modelling to produce **RM maps** (***MIRG***).
  b. We have also gone a step further using **local-constrained cosmological Magneto-Hydro-Dynamical** (***MHD***) **simulations** (***SLOW***), which provide **significant improvements** in **realistic ICM** modelling in a **cosmological context.**
- **Bayesian model selection** analysis to determine which **magnetic field amplification mechanism is consistent** with the **data**.

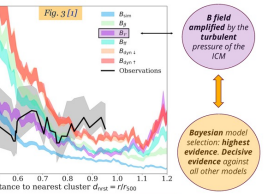
4. Results

- **First detection of magnetised gas in the SSC from the excess RM scatter:**

$$\sigma_{\mathrm{RM}}^{\mathrm{SSC}} = 30.5 \pm 4.6\ \mathrm{rad/m^2}$$ ⟺ **7σ statistical significance!**

- From the *SLOW* **cosmological MHD simulations we have obtained:**
  - **SSC system *replica*** constrained to Local Universe observations *(Fig. 2 a)*.
  - **RM maps** for different **magnetic field amplification mechanisms** in the intercluster region *(Fig. 2 b)*.
  - **RM scatter profiles** with respect to the **distance to the** centres of the **clusters** $\mathcal{S}_{\mathrm{RM}}$ *(Fig. 3)*.





***B* field amplified** by the **turbulent** pressure of the ICM

Bayesian model selection: **highest evidence**. **Decisive evidence** against all other models

5. Conclusions

- **SKA pathfinder radio telescopes** provide **high-quality data** to **detect magnetic fields** in the Universe through **Faraday rotation**.
- **First detection** of an excess **RM signal** from the **SSC** is **consistent with ~μG magnetic field strengths ↔ agreement** with **previous studies** of other clusters of galaxies.
- The **data favors** models in which **magnetic field** in the **intercluster regions** is **amplified** by the **turbulent pressure of the ICM**.
- However, the **trend** of the SSC RM signal **with distance to the clusters** is **flatter than** current **most accurate modelling** *(see Fig. 3)*.
  - Observational bias? Better modelling?

References

[1] *Alonso-López et al. 2025 (A&A, under review)*
[2] *Guenster, B. M., et al. 2025*

Acknowledgements

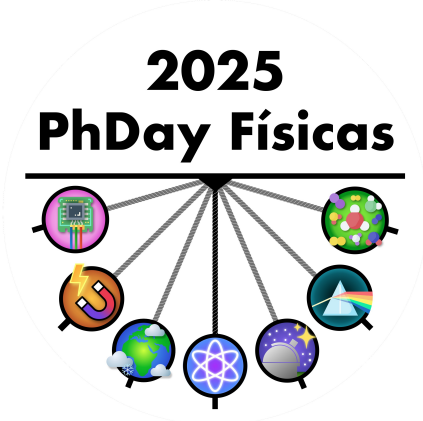
FACULTAD DE CIENCIAS FÍSICAS

2

Estudio de los precursores estratosféricos de eventos extremos en superficie a través de la modelización climática

Daniel De Maeseneire Martínez

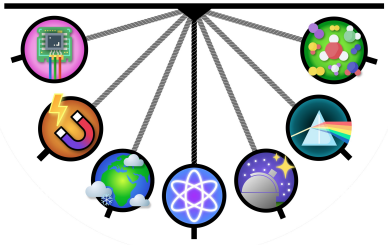
ESCUELA DE DOCTORADO
UNIVERSIDAD COMPLUTENSE DE MADRID



2

Nombre	Daniel
Apellidos	De Maeseneire Martínez
Departamento	FTA
Doctorado	Física
Director/es de la Tesis	Blanca Ayarzagüena, Natalia Calvo
Título de la contribución	***Estudio de los precursores estratosféricos de eventos extremos en superficie a través de la modelización climática***

2025 PhDay Físicas



Are SSW impacts on surface temperature extremes changing due to increasing CO_2 concentrations?

Daniel De Maeseneire[1], Blanca Ayarzagüena[1], Natalia Calvo[1]

[1] Earth Physics and Astrophysics Department, Universidad Complutense de Madrid, Madrid, Spain

2025 PhDay Físicas

1 – Motivation

Sudden stratospheric warmings (SSWs) are extreme disruptions of the wintertime polar circulation (polar vortex) that can **alter the tropospheric weather for over two months**[1] and potentially influence the occurrence of **surface extreme events**[2].

Climate models show great **uncertainty** in how the stratospheric polar vortex is going to change in the future due to the CO_2 increase[3] with **opposite response of the SSWs frequency** to CO_2[4].

Is the SSWs-troposphere connection going to change in the future? Are these changes model dependent?

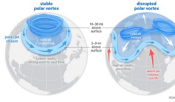


Figure 1: Illustration of the stratospheric polar vortex a) stable polar vortex b) disrupted polar vortex when a Sudden Stratospheric Warming happen. Figure from NOAA https://www.noaa.gov/

2 – Data & Methods

- **12 CMIP6 climate models:**
  - High top models
  - Simulations used: pre-industrial conditions (**piControl**) vs quadrupling CO_2 concentrations (**abrupt4xCO_2**)
- **Climate models classification:**

Based on the sign of the change in SSWs frequency

Models with a negative change in SSWs (NEG)

Models with a positive change in SSWs (POS)

3 – Stratosphere-troposphere connection during SSWs

3.1 Downward propagation of the stratospheric signal:

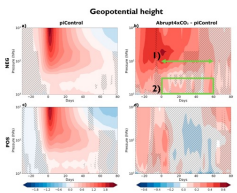


Figure 2: Standardized geopotential height anomalies for the polar cap (65°–90°) for SSWs composites from (-30:60) days relative to the onset. (a,c) piControl simulation for multimodel mean NEG and POS models respectively. (b,d) abrupt4xCO_2 – piControl simulation for multimodel mean NEG and POS models. Stripes represent non-statistically significant values.

The **lower stratosphere (100 hPa)** is highly relevant for the stratosphere-troposphere coupling and the amplitude of SSW surface impacts.

The SSW signal is similar in the piControl simulation for both **NEG** and **POS** models. We found an **opposite response** to the CO_2 increase between the two model groups.

There is **stronger** downward propagation in **NEG models** in the abrupt4xCO_2 (Figure 2):

1) More persistence at 100hPa
2) Stronger signal reaching surface

3.2 SSWs Surface impacts:

Sea level pressure: Near-surface circulation anomalies **intensify due to increased CO_2** in the North Atlantic region particularly in **NEG models**.

Surface temperature: SSW impacts on do not change except for Barent—Kara Sea where sea ice loss could be heavily affected.

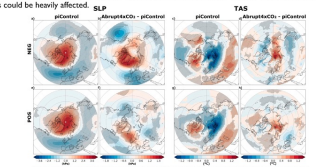


Figure 3: Composites of averaged SLP anomalies (shading, hPa) over days (0:60) relative to the SSWs onset for the multimodel mean for piControl simulation for (Top row) NEG models and (Bottom row) POS models and Differences abrupt4xCO_2, minus piControl

Larger differences in SLP and TAS in **NEG models** that show **stronger SSWs surface impacts** as a response to the CO_2 increase (Figure 3):

4 – SSW and Surface temperature extreme events

Scandinavian cold spells:

Scandinavia is where the Canonical response of SSWs is located as the SLP pattern resembles the SSWs response (Figure 4).

It is the region most affected by the SSWs impacts and **~1/3 of cold spells** are preceded by an SSW.

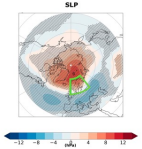


Figure 4: Composites of SLP anomalies for SSWs-related cold spells duration in Scandinavia in the piControl simulation for c) NEG models and f) POS models. Stripes represent significant values at a 95% confidence level.

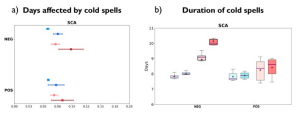


Figure 5: a) Probability of days affected by a surface extreme event in Scandinavia. Bars represent ±1 standard deviation. b) Boxplots of the multimodel distribution of surface extreme event duration

Pre-Industrial:

- There is an **increased risk (~25%)** in the probability of occurrence of cold spells after an SSW
- Cold spells with SSWs **tend to be more persistent** but the difference is not statistically significant

Response to 4xCO_2:

- The probability of cold spells increases even more in **NEG models**
- Cold spells are more persistent after an SSW specially in **NEG models** where the duration is up to **10 days**

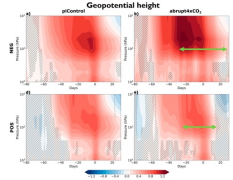


Figure 6: Composite maps of standardized geopotential height anomalies for the polar cap (65°-90°N) for SSWs-related cold spells duration in Scandinavia (-30, 30) days relative to the onset of the extremes. Panels (a, c) show results from the piControl simulation and (b, e) for abrupt4xCO_2 simulation for the multimodel mean of NEG and POS models, respectively. Stripes represent non-significant values at a 95% confidence level.

The favorable conditions for cold spells following SSWs are intensified due to CO_2 increase, especially in **NEG models** where the downward propagation is stronger (Figure 6)

5 – Conclusions

- The sign of the change in the SSW frequency also affects the downward propagation of their signal under increased CO_2 concentrations. **NEG models** simulate a larger persistence of the SSW anomalies in the lower stratosphere in the *abrupt4xCO_2* run compared to the *piControl*, leading to a stronger signal reaching the surface.
- SSWs favor the occurrence of days affected by cold spells over the Scandinavian region. They also tend to prolong the duration of these extremes. These impacts are larger for **NEG models** in the abrupt4xCO2 simulation where there is a stronger downward propagation of the SSW signal caused by the larger persistence in the lower stratosphere.

6 – References

[1] Baldwin, M. P., Ayarzagüena, B., Birner, T., Butchart, N., Butler, A. H., Charlton-Perez, A. J., et al. (2021). 60S Sudden Stratospheric Warmings. Reviews of Geophysics, 59(1).

[2] Domeisen, D. I. V., & Butler, A. H. (2020). Stratospheric drivers of extreme events at the Earth's surface. 641 Communications Earth and Environment: Nature Publishing Group.

[3] Karpechko, A. Y., Afargan-Gerstman, H., Butler, A. H., Domeisen, D. I. V., Kretschmer, M., Lawrence, Z., et al. 911 al. (2022). Northern Hemisphere Stratosphere-Troposphere Circulation Change in CMIP6 Models: 1. Inter-912 Model Spread and Scenario Sensitivity. Journal of Geophysical Research: Atmospheres, 127(19).

[4] Ayarzagüena, B., Charlton-Perez, A. J., Butler, A. H., Hitchcock, P., Simpson, I. R., Polvani, L. M., et al. 786 (2020). Uncertainty in the Response of Sudden Stratospheric Warmings and Stratosphere-Troposphere 787 Coupling to Quadrupled CO2 Concentrations in CMIP6 Models. Journal of Geophysical Research: 788 Atmospheres, 125(5).

De Maeseneire, D., Ayarzagüena, B., Calvo, N. On the changes in the connection between SSWs and Surface extreme weather in response to an abrupt 4xCO2 increase. *Journal of Geophysical Research*. **(under review)**

FACULTAD DE CIENCIAS FÍSICAS

3

Depósito de Capas Nanométricas de AZO por Sputtering de Alta Presión: Caracterización y Aplicación en Células Solares de Alta Eficiencia

Sebastián Duarte Cano

ESCUELA DE DOCTORADO
UNIVERSIDAD COMPLUTENSE DE MADRID

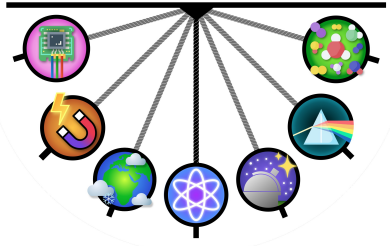
2025 PhDay Físicas



3

Nombre	Sebastián
Apellidos	Duarte Cano
Departamento	EMFTEL
Doctorado	Física
Director/es de la Tesis	Rodrigo García Hernansanz
Título de la contribución	***Depósito de Capas Nanométricas de AZO por Sputtering de Alta Presión: Caracterización y Aplicación en Células Solares de Alta Eficiencia***

2025 PhDay Físicas



ALUMINUM ZINC OXIDE LAYERS BY HIGH-PRESSURE SPUTTERING FOR SOLAR CELLS APPLICATION.

2025 PhDay Físicas

S. Duarte-Cano[1*], R. García-Hernansanz[1], F. Pérez-Zenteno[1], R. Benítez-Fernandez[1], I. Martil[1] E. García-Hemme[1], J. Olea[1], D. Pastor[1], A. del Prado[1], E. San Andrés[1], S. Algaidy[2]

[1]Dpto. EMFTEL, Fac. CC. Físicas, Univ. Complutense de Madrid, 28040, Madrid, Spain; *seduarte@ucm.es.

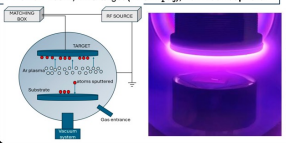
[2] Instituto de Energía Solar, Universidad Politécnica de Madrid, E.T.S.I. Telecomunicación, 28040 Madrid, Spain

MOTIVATION

- **ITO limitations:** High cost and scarcity of indium restrict large-scale use of ITO in transparent electrodes.
- **AZO advantages:** Aluminum-doped ZnO is abundant, low-cost, non-toxic, highly transparent, and combines good conductivity with stability.
- **Common AZO deposition methods**: low-pressure magnetron sputtering, Pulsed Laser Deposition (PLD), or Chemical Vapor Deposition (CVD).
- **High-pressure sputtering (HPS):** At mbar pressures, thermalized species reduce substrate damage and enable dense, conductive films even at low substrate temperatures. $\lambda = \frac{kT}{\sqrt{2}\pi d^2 p}$

EXPERIMENTAL

- Sputtering pressure: **0.46-2.2 mbar**
- **Power:** 100W, **AZO** target (**ZnO/Al_2O_3**), **x6 Ar atmosphere**

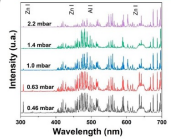


Characterization techniques

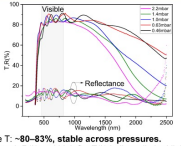
- OES✓
- Ellipsometry ✓
- Transmittance ✓
- Reflectance ✓
- XPS ✓
- GIXRD ✓
- AFM ✓
- Resistivity ✓
- Carrier concentration ✓
- Mobility✓

RESULTS

OPTICAL EMISSION SPECTROMETRY

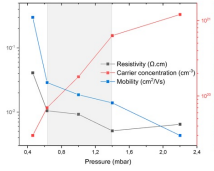


TRANSMITTANCE & REFLECTANCE



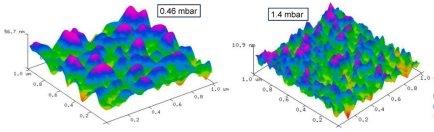
- Average T: ~**80–83%, stable across pressures.**
- Low, smooth R(Å) and high flat T(Å) indicate limited light scattering, **consistent with a dense, low-roughness AZO film** suitable for TCO use.

ELECTRICAL CHARACTERIZATION



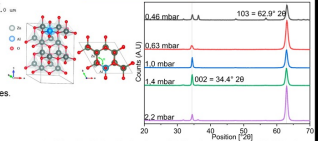
- Carrier concentration **increases with pressure,** leading to higher conductivity. Increased collisions between carriers, **decreasing mobility (μ).**
- Higher pressures promote the formation of more defects in the film, leading to a **decrease in carrier mobility**

ATOMIC FORCE MICROSCOPY



- Roughness decreases from 0.46 → 1.0–1.4 mbar, yielding more uniform, high-quality films.
- Optimal window: 1.0–1.4 mbar (smooth, dense morphology; controlled growth).
- *At 2.2 mbar the roughness increases → deposition becomes less controlled, not ideal for smooth surfaces.

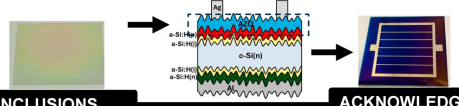
X-RAY DIFFRACTION



- Wurtzite ZnO with dominant (002) at 34.4°, (103) at 62.9° is also present.
- Coincidence of the peaks with the expected positions corresponds to the **hexagonal wurtzite phase**, typical of AZO
- (002) texture strengthens around 0.63–1.0 mbar, indicating better c-axis orientation.

Pressure (mbar)	Resistivity (Ω.cm)	T(m) (%)	μ (cm²/Vs)	n(cm⁻³)	E_{gap} (eV)
0.46	4.1×10^{-2}	79.7	8.3	3.0×10^{19}	3.41
0.63	1.1×10^{-2}	82.6	5.1	7.0×10^{19}	3.45
1.0	9.3×10^{-3}	82.9	4.5	1.8×10^{20}	3.47
1.4	5.1×10^{-3}	79.7	4.1	6.3×10^{20}	3.52
2.2	6.5×10^{-3}	78.3	2.5	1.2×10^{21}	3.60
Ref. Value (0.001–0.012)	~1×10^{-3}	80-92	10-35	3×10^{19} - 5×10^{20}	3.35-3.70

FROM AZO FILM TO SOLAR CELL: DEPOSITION, INTEGRATION, DEVICE



➢ **Published Work!** Scan QR code

CONCLUSIONS

- We have deposited AZO using High-Pressure Sputtering (HPS), and the resulting films are **suitable for use in solar cells**
- In the pressure range of **0.63 mbar to 1 mbar**, the films produced show a favorable balance between low resistivity, high transmittance, adequate roughness and optimal AZO properties.

ACKNOWLEDGEMENT

The authors would like to acknowledge the "CAI de Técnicas Físicas, for the collaboration at various stages of this research, including measurements and characterization. This project was funded by AEI through the projects PID2020-116508RB-I00, PID2023-149369OB-C21 and TED2021-130894B-C21, and by the Comunidad Autonoma de Madrid through the project PR37/24 TEC-2024/ECO-72 F. Pérez-Zenteno acknowledges the predoctoral contract from UCM (call CT58/21-CT59/21) . R. Benítez-Fernández acknowledges the predoctoral contract from Comunidad Autónoma de Madrid (PIPF-2023/ECO-30541).

References

[1] S. Duarte-Cano et al., (2025),10.1016/j.apsusc.2025.164357.

[2] D. Caudevilla et al., (2022). 10.1016/j.mssp.2021.106189

[3] F. Pérez-Zenteno et al, (2025). 10.1016/j.mssp.2024.109038

FACULTAD DE CIENCIAS FÍSICAS

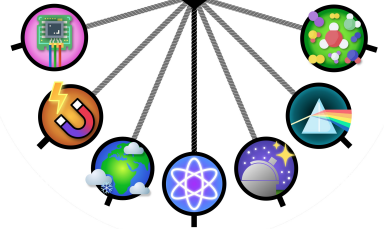
4

Performance of an impact-based Earthquake Early Warning System in the Alboran Sea

Lucía Escudero Palencia

ESCUELA DE DOCTORADO
UNIVERSIDAD COMPLUTENSE DE MADRID

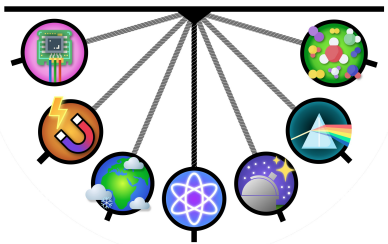
2025 PhDay Físicas



4

Nombre	Lucía
Apellidos	Escudero Palencia
Departamento	FTA
Doctorado	Física
Director/es de la Tesis	Maurizio Mattesini y Aldo Zollo
Título de la contribución	***Performance of an impact-based Earthquake Early Warning System in the Alboran Sea***

2025
PhDay Físicas



Performance of an impact-based Earthquake Early Warning System in the Alboran Sea

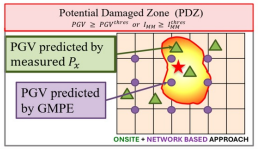
2025 PhDay Físicas

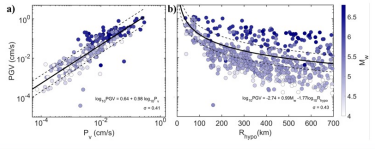
ESCUDERO, Lucía[1]; **MATTESINI, Maurizio**[1,3]; **ZOLLO, Aldo**[2]; **REA, Raffaele**[2]; **ELIA, Luca**[2,4]; **COLOMBELLI, Simona**[2] and **BUFORN, Elisa**[1,3]

[1] Departamento de Física de la Tierra y Astrofísica, Facultad de Ciecias Físicas, Universidad Complutense de Madrid, Spain; [2] Dipartimento di Fisica "Ettore Pancini", Università degli Studi di Napoli Federico II, Italy; [3] Facultad de Ciencias Físicas, Instituto de Geociencias (UCM-CSIC), Spain; [4] Istituto Nazionale di Geofisica e Vulcanologia, Sezione di Napoli Osservatorio Vesuviano, Italy

1. Introduction

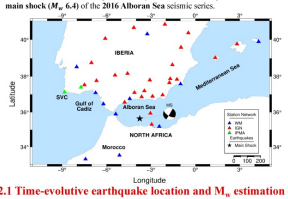
We implemented a **P-wave shaking-forecast-based Earthquake Early Warning System (EEWS)** method in the **Ibero-Maghrebian Region (IMR),** using real-time mapping of the **Potential Damage Zone (PDZ)**-the epicentral area where the **Peak Ground Velocity (PGV)** is predicted to exceed a pre-set threshold during an earthquake (Zollo *et al.*, 2023). This method uses ***QuakeUp*** software, developed by the ***RISSC-Lab***[*]. PGV values are converted to Instrumental Intensity (I_{MM}) using the Faenza & Michelini (2010) empirical relation (MCS scale), generating an I_{MM} **shake map** that updates over time to monitor the PDZ.





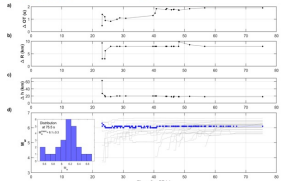
2. Offline testing of the EEWS performance

Here we illustrate the **retrospective analysis** of the method's performance for the **main shock (M_w 6.4)** of the **2016 Alboran Sea** seismic series.

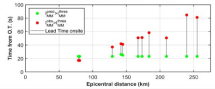


2.1 Time-evolutive earthquake location and M_w estimation

As the P-wave is detected at **5 stations**, a **probabilistic and time-evolving location and magnitude estimation** are performed using ***RTLoc*** **algorithm** (Satriano *et al.*, 2008) and the method of Zollo *et al.*, 2023, respectively.



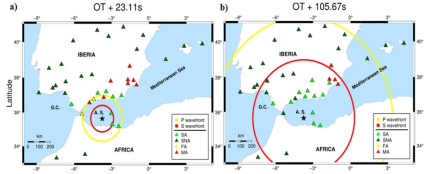
2.2. Lead-Time ($I_{MM}^{thres} = IV$)



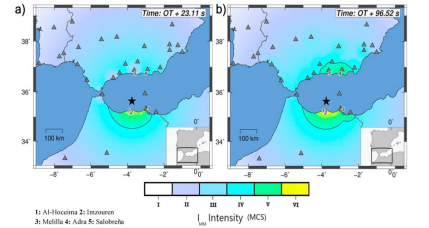
2.3. Quality of the impact prediction ($I_{MM}^{thres} = IV$)

The **accuracy of impact prediction** is assessed by applying the decision matrix of Zollo *et al.*, (2023):

- **Successful Alerts (SA):** $I_{MM}^{pred} \geq I_{MM}^{thres}$ & $I_{MM}^{obs} \geq I_{MM}^{thres}$
- **Successful No-Alerts (SNA):** $I_{MM}^{pred} < I_{MM}^{thres}$ & $I_{MM}^{obs} < I_{MM}^{thres}$
- **Missed Alerts (MA):** $I_{MM}^{pred} < I_{MM}^{thres}$ & $I_{MM}^{obs} \geq I_{MM}^{thres}$
- **False Alert (FA):** $I_{MM}^{pred} \geq I_{MM}^{thres}$ & $I_{MM}^{obs} < I_{MM}^{thres}$



2.4. P-wave based shake maps. Potential Damage Zone ($I_{MM}^{thres} = V$)



1: Al-Hoceima 2: Imzouren
3: Melilla 4: Adra 5: Salobreña

3. Conclusions

- We **implemented and tested a new P-wave shaking-forecast-based EEWS**, called ***QuakeUp***, at the IMR. It has proven effective for moderate-magnitude offshore earthquakes in the IMR.
- We **calibrated region-specific relationships** between PGV and P-wave peak amplitudes (acceleration, velocity, and displacement), as well as between magnitude and P-wave peak amplitudes. A GMPE $M_w \geq 4$ earthquakes in the IMR was developed.
- For $I_{MM}^{thres} = IV$, the **lead-time ranges from 14 to 62 s**, which increases with the epicentral distance (up to 260 km). The accuracy of the impact prediction improves over time.

[*] ***RISSC-Lab:*** Unità di **R**icerca in **S**ismologia **S**perimentale e **C**omputazionale, Università degli Studi di Napoli Federico II (Italy)

References

Buforn *et al.*, (2017): http://dx.doi.org/10.1016/j.tecto.2017.06.033
Escudero *et al.*, (2025): https://doi.org/10.1785/0220240474
Faenza & Michelini (2010): https://doi.org/10.1111/j.1365-246X.2009.04467.x
Satriano *et al.*, (2008): https://doi.org/10.1785/0120060159
Zollo *et al.*, (2023): https://doi.org/10.1029/2022EA002657

Acknowledgments

This work has been partially supported by the **Spanish Ministry of Economy and Competitiveness** (Project Number PID2021-123626OB-I00) and the **Geo-INQUIRE project** funded by the European Commission (HORIZON-INFRA-2021-SERV-01, Project Number 101058518).

FACULTAD DE CIENCIAS FÍSICAS

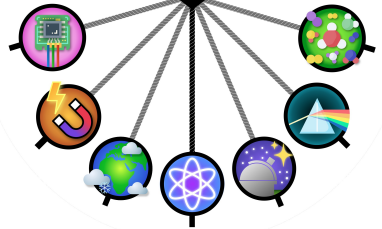
5

Electron hydrodynamics in graphene devices

Jorge Estrada Álvarez

ESCUELA DE DOCTORADO
UNIVERSIDAD COMPLUTENSE DE MADRID

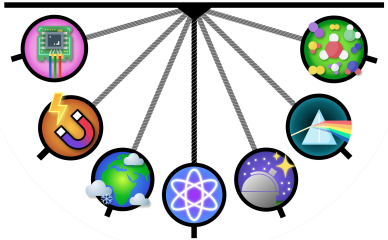
2025 PhDay Físicas



5

Nombre	Jorge
Apellidos	Estrada Álvarez
Departamento	FM
Doctorado	Física
Director/es de la Tesis	Elena Díaz García, Francisco Domínguez-Adame Acosta
Título de la contribución	***Electron hydrodynamics in graphene devices***

2025
PhDay Físicas



Electron hydrodynamics in graphene devices

J. Estrada-Álvarez. Supervisors: E. Díaz, F. Domínguez-Adame. GISC Departamento de Física de Materiales UCM

2025 PhDay Físicas



Electronic transport in graphene defies Ohm's law and gives rise to hydrodynamic signatures: electronic whirlpools, tunable differential resistance for terahertz applications, and superballistic conduction, which reduces device dissipation. The hydrodynamic signatures highlight the relevance of the device's geometry.

Why is geometry so important?

Momentum-relaxing collisions no longer dominate.



For each defect ×2 edge collisions ×4 electron-electron

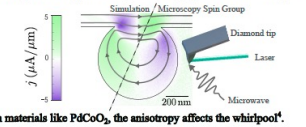
The Boltzmann model replaces Ohm's law, and, in the hydrodynamic limit, electrons obey the Stokes-Ohm equation[1-3]

$$-\nu\nabla^2\boldsymbol{u}+\frac{v_F}{l_{\rm mr}}\boldsymbol{u}=\frac{ev_F}{\hbar k_F}\nabla V.$$

If the flow is inhomogeneous, the viscosity *wakes up*.

Electronic whirlpools

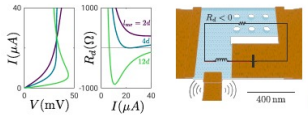
Whirlpools are a signature of non-ohmic transport. Quantum sensing with nitrogen-vacancy microscopy provides direct images.



In materials like $PdCoO_2$, the anisotropy affects the whirlpool[4].

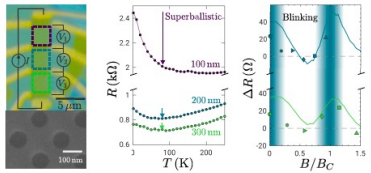
Terahertz technology

The electron viscosity decreases with current. The negative differential resistance enables amplifiers and oscillators[5].



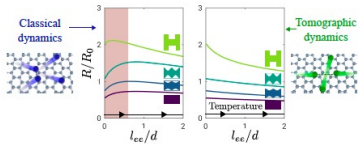
Superballistic conduction

An antidot superlattice bends the electron flow and boosts hydrodynamics[4].



Reduced dissipation

Optimizing the device's geometry, together with electron-electron collisions, reduces resistance[7]. Tomographic dynamics for the electron collisions solve the ***superballistic paradox*** and further reduce the resistance[8].



The geometry determines the electrical properties. The antidot lattice enhances hydrodynamics.

Phenomena without an analog in conventional fluids: magnetic fields, anisotropy, and tomographic dynamics.

Hydrodynamics enables terahertz technology and optimized devices with reduced energy dissipation.

We acknowledge J. Salvador-Sánchez, A. Pérez, M. Amado, E. Diez; C. Ding, C. Degen for NV imaging; R. Brito and F. Bermúdez-Mendoza for discussions. Funded by the "(MAD2D-CM)-UCM" by Comunidad de Madrid, the Recovery, Transformation, and Resilience Plan, and by NextGenerationEU from the EU and AEI (PID2022-136285NB-C31), and M. Ciencia, Innovación y Universidades (Grant FPU22/01039).

1 J. Estrada-Álvarez *et al.* Comm. Phys. **7**, 138 (2024).
2 J. Estrada-Álvarez *et al.* Rev. Esp. Fís. **38**, 12 (2024).
3 J. Estrada-Álvarez *et al.* Sci. Rep. [accepted for publication].
4 J. Estrada-Álvarez *et al.* Phys. Rev. Res. **7**, 013087 (2025).
5 J. Estrada-Álvarez *et al.* 2D Mater. **12**, 015012 (2024).
6 J. Estrada-Álvarez *et al.* Phys. Rev. X **15**, 011039 (2025).
7 J. Estrada-Álvarez *et al.* Phys. Rev. B **111**, 075401 (2025).
8 J. Estrada-Álvarez *et al.* Phys. Rev. Lett. [accepted for publication].

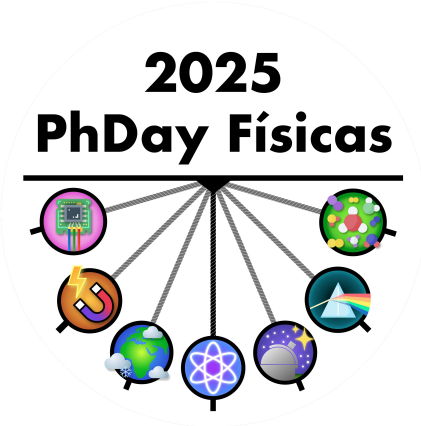
FACULTAD DE CIENCIAS FÍSICAS

6

Insights into the 100 largest European surface ozone episodes during spring–summer 2003–2022

Tahimy Fuentes Alvarez

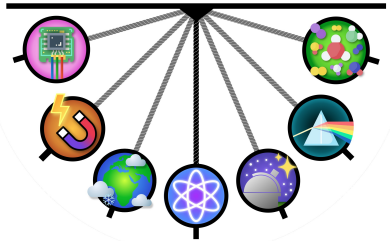
ESCUELA DE DOCTORADO
UNIVERSIDAD COMPLUTENSE DE MADRID



6

Nombre	Tahimy
Apellidos	Fuentes Alvarez
Departamento	FTA
Doctorado	Física
Director/es de la Tesis	Carlos Ordóñez
Título de la contribución	***Insights into the 100 largest European surface ozone episodes during spring–summer 2003–2022***

2025
PhDay Físicas



Factores meteorológicos e incertidumbres en las proyecciones climáticas del ozono superficial en Europa

Tahimy Fuentes-Alvarez[1], Carlos Ordóñez[1], Ricardo García-Herrera[1,2], David Barriopedro[2]

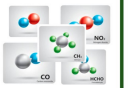
1 Universidad Complutense de Madrid, Departamento de Física de la Tierra y Astrofísica
2 Instituto de Geociencias, UCM-CSIC

2025 PhDay Físicas

MOTIVATION

Tropospheric ozone (O_3) forms through complex photochemical reactions involving precursors such as nitrogen oxides, non-methane volatile organic compounds, carbon monoxide, and methane in the presence of sunlight.

O_3 is highly dependent on solar radiation, temperature (Otero et al., 2016) and land use changes.



CURRENT SCIENTIFIC CONSENSUS

Future ozone concentrations will be determined by changes in both climate and precursor emissions:

- A warmer atmosphere can lead to local O_3 increases during the peak season in polluted regions.
- Efforts to control precursor emissions are expected to yield O_3 reductions.

DATA & METHODS

Chemical data:
- CAMS reanalysis
  - 1.0° x 1.0° horizontal resolution
  - Daily (April–May 2003–2022)
- CAMS global emission inventory dataset



Fig. 1: Output of the ozone episode detection algorithm

Semi-Lagrangian algorithm

Meteorological data
- ERA5 reanalysis
- T2M, Z500, precipitation, wind speed, ω500
- Same horizontal and temporal resolution



Air stagnation Index (ASI)



Blocks and ridges algorithm



Additional data:
- GFAS → Wildfire radiative power

Regional projection index

$$I(Z500)^R = \frac{< Z500_{daily}, Z500^R >}{< Z500^R, Z500^R >}$$

Flow analogues
- (e.g. Yiou et al. 2014)

(Sousa et al 2021)

Meteorological conditions and dynamical processes contributing to high ozone levels vary across regions

SOUTHERN HALF OF BRIT:
- **Advection** of clean air masses.
- Strong winds ventilate the region, reducing precursors levels, thereby limiting ozone titration by NO.

EEU:
- **Anticyclonic conditions**
- **High emissions of ozone precursors** from wildfires.

NORTHERN PART OF CEU:
- **anticyclonic conditions**
- high Z500 and T2M anomalies
- reduced wind and precipitation deficits

SOUTHERN PART OF CEU:
- modest positive anomalies of T2M and Z500
- weak winds
- **enhanced subsidence.**

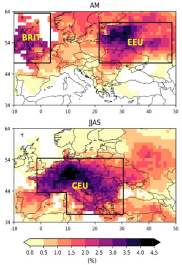
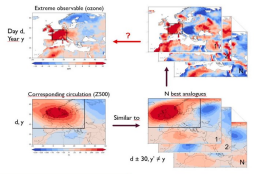


Fig. 1: Frequency of occurrence (% over the total number of days) of the 100 largest European ozone episodes during April–May (AM, top) and June–September (JJAS, bottom) of 2003–2022. The boxes indicate the location of the regions with the highest incidence of episodes: British Isles (BRIT) and eastern Europe (EEU) in AM and central Europe (CEU) in JJAS.

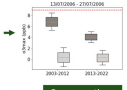
As we understand the associated mechanisms of regional ozone episodes ...

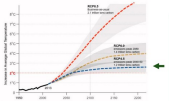
PAST

... we can better estimate the evolution of ozone in the future based on different climate scenarios?



Under similar meteorological forcing, ozone has decreased over time in line with the decrease in pollutant emissions.





Open questions
- Which process will control the occurrence of ozone extremes in the future: climate change or precursor emissions?
- How extreme will ozone levels be in the future?

FUTURE

HIGHLIGHTS

- The processes contributing to high ozone levels vary across regions in Europe.
- Weather forcing plays an important role in the occurrence of ozone episodes.
- For similar weather conditions, ozone concentrations have decreased in line with the reduction in precursor emissions.
- Using the analogue method, we can estimate the role of climate change and precursor emissions in the occurrence of ozone extremes in the future.

REFERENCES

Otero, N., Sillmann, J., Schnell, J. L., Rust, H. W., & Butler, T. (2016). Synoptic and meteorological drivers of extreme ozone concentrations over Europe. *Environ. Res. Lett., 11*, 024005. https://doi.org/10.1088/1748-9326/11/2/024005

Sousa, P. M., Barriopedro, D., García-Herrera, R., Woollings, T., & Trigo, R. M. (2021). A New Combined Detection Algorithm for Blocking and Subtropical Ridges. J. Clim., 34(18), 7735–7758. https://doi.org/10.1175/JCLI-D-20-0658.1

Yiou P, Bastos M, Vautard R, Vrac M, Jourdain S, Garnier E, Flateau P, Mercul L (2014). Ensemble meteorological reconstruction using circulation analogues of 1781–1785. Clim Past 10(2):797–809. doi:10.5194/cp-10-797-2014

Acknowledgements. Predoctoral fellowship PRE2022-101985 and MALONE project (PID2021-122252OB-I00), funded by Spanish Ministry of Science and Innovation.

Tahimy Fuentes-Alvarez, Carlos Ordóñez, Ricardo García-Herrera, David Barriopedro, Rodrigo Crespo-Miguel, Miguel M. Lima (2025). Insights into the 100 largest European surface ozone episodes during spring–summer 2003–2022, Science of The Total Environment,1001,180578, https://doi.org/10.1016/j.scitotenv.2025.180578.

FACULTAD DE CIENCIAS FÍSICAS

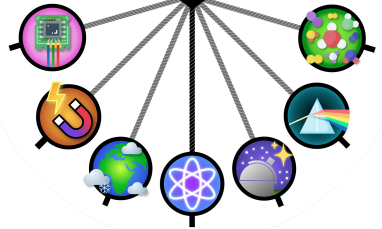
7

Orientation-Tuned Hall Responses in Strongly Correlated Oxide Heterostructures

Rafael Fuster Rico

ESCUELA DE DOCTORADO
UNIVERSIDAD COMPLUTENSE DE MADRID

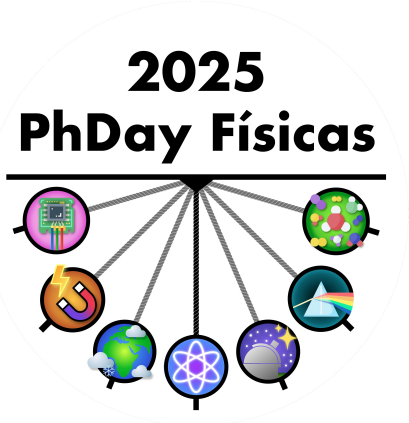
2025 PhDay Físicas

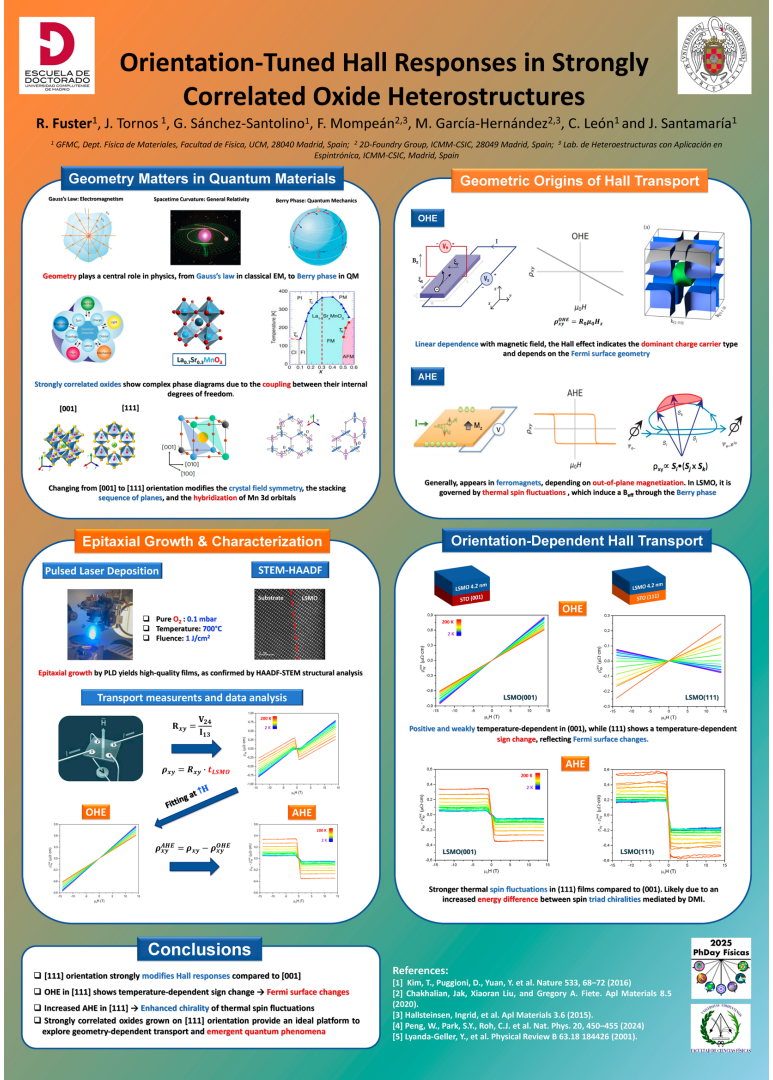


7

Nombre	Rafael
Apellidos	Fuster Rico
Departamento	FM
Doctorado	Física
Director/es de la Tesis	Javier Tornos Castillo y Jacobo Santamaría Sánchez-Barriga
Título de la contribución	***Orientation-Tuned Hall Responses in Strongly Correlated Oxide Heterostructures***

2025 PhDay Físicas





FACULTAD DE CIENCIAS FÍSICAS

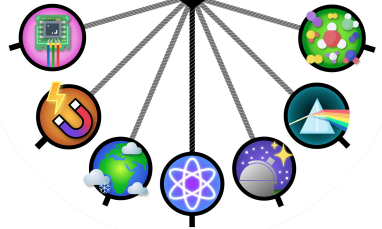
8

Quantum Simulations of QCD within a particle-based codification

Juan José Gálvez Viruet

ESCUELA DE DOCTORADO
UNIVERSIDAD COMPLUTENSE DE MADRID

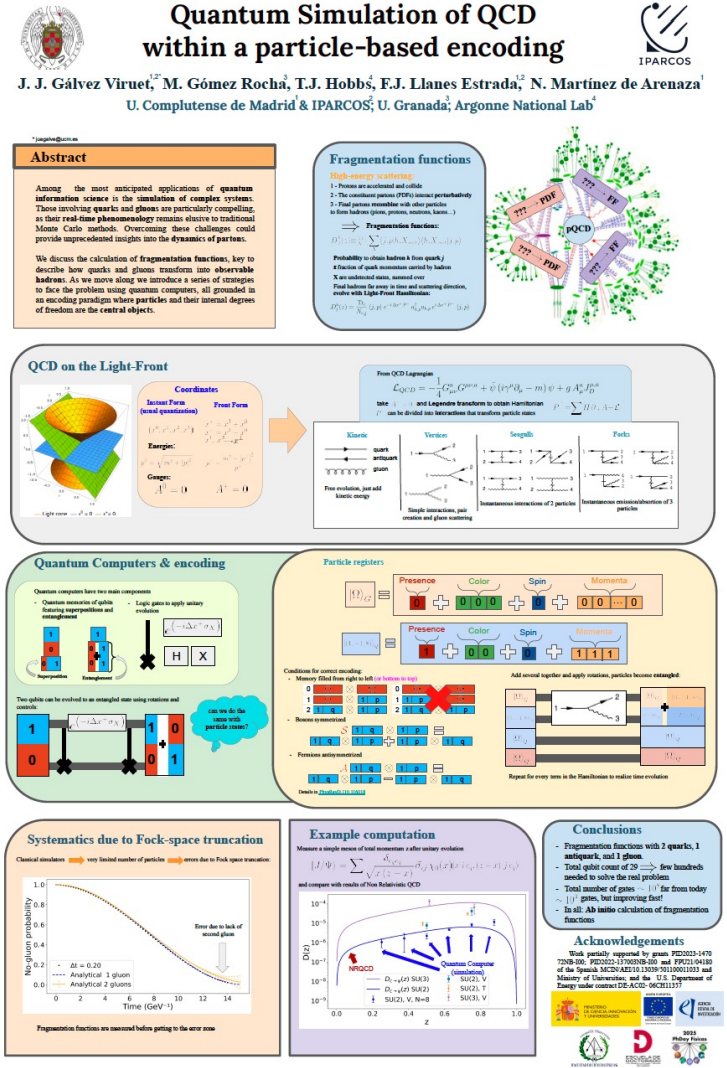
2025 PhDay Físicas



8

Nombre	Juan José
Apellidos	Gálvez Viruet
Departamento	FT
Doctorado	Física
Director/es de la Tesis	Felipe J. Llanes Estrada y María Gómez Rocha
Título de la contribución	***Quantum Simulations of QCD within a particle-based codification***

2025
PhDay Físicas



FACULTAD DE CIENCIAS FÍSICAS

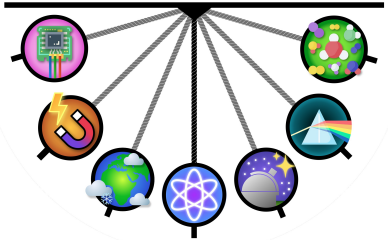
9

Sputter-deposited Nanocolumns: Tuning Fe and Au Properties for In Vitro Biomedical Applications

María Garrido Segovia

ESCUELA DE DOCTORADO
UNIVERSIDAD COMPLUTENSE DE MADRID

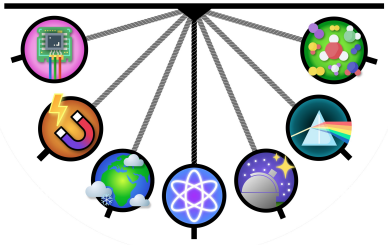
2025 PhDay Físicas



9

Nombre	María
Apellidos	Garrido Segovia
Departamento	FM
Doctorado	Física
Director/es de la Tesis	Elena Navarro Palma, José Miguel García Martín y Ana Espinosa de los Monteros Royo
Título de la contribución	***Sputter-deposited Nanocolumns: Tuning Fe and Au Properties for In Vitro Biomedical Applications***

2025 PhDay Físicas



Sputter-deposited Nanocolumns: Tuning Fe and Au Properties for In Vitro Biomedical Applications

María Garrido-Segovia[1*], Elena Navarro[1,2], Ana Espinosa[3] and José Miguel García-Martín[4]

[1]Departamento de Física de Materiales, Universidad Complutense de Madrid (UCM), Madrid, Spain
[2]Instituto de Magnetismo Aplicado (IMA-UCM-ADIF), Las Rozas de Madrid, Madrid, Spain
[3]Instituto de Ciencia de Materiales de Madrid, CSIC (CEI UAM+CSIC), Cantoblanco, Madrid, Spain
[4]Instituto de Micro y Nanotecnología, IMN-CNM, CSIC (CEI UAM+CSIC), Tres Cantos, Madrid, Spain

*magarr11@ucm.es

2025 PhDay Físicas

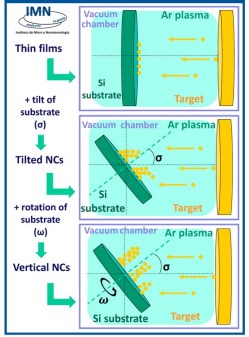
Motivation

Sputtering is a widely used technique in industry for the production of homogeneous thin films. The versatility of this technique also enables the growth of nanocolumnar structures to be made of a variety of materials by tilting the substrate during atomic deposition [1]. The nanostructuring of Au facilitates the development of systems that exhibit a Localized Surface Plasmon Resonance (LSPR), which enables their application in photothermal therapy, as well as the integration of Fe allows for the creation of hyperthermic agents [2]. The strategic combination of both materials yields a synergetic system that is highly advantageous for various biomedical applications, as well as in magnetoplasmonics [3].

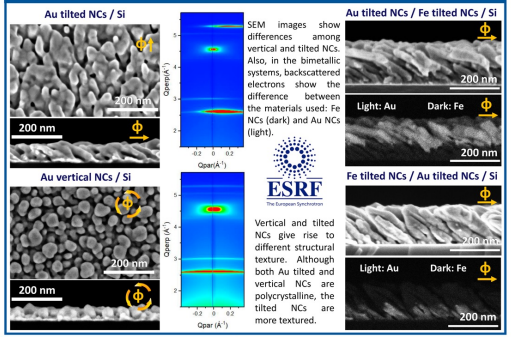
Objectives

Four morphologies of Au and Au/Fe nanocolumns (NCs) have been grown on a silicon substrate: i) **Au tilted NCs**, ii) **Au vertical NCs**, iii) **Fe tilted NCs on Au tilted NCs** and iv) **Au tilted NCs on Fe tilted NCs**. The nanocolumns have been extensively characterized through **SEM** (morphological characterization), **XRD** (structural characterization at the European Synchrotron Radiation Facilities, ESRF), **reflectivity** (plasmonic studies) and **VSM** (magnetic characterization). Most importantly, **viability** and **adhesion** measurements have been carried out to determine if these systems are suitable for *in vitro* studies for biomedical applications, which is the main objective of this work.

Growth of the nanocolumns: MS-GLAD



Morphological and structural characterization: SEM & XRD (ESRF)



SEM images show differences among vertical and tilted NCs. Also, in the bimetallic systems, backscattered electrons show the difference between the materials used: Fe NCs (dark) and Au NCs (light).

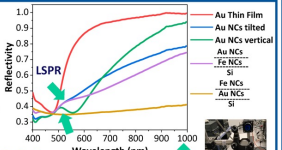
ESRF

Vertical and tilted NCs give rise to different structural texture. Although both Au tilted and vertical NCs are polycrystalline, the tilted NCs are more textured.

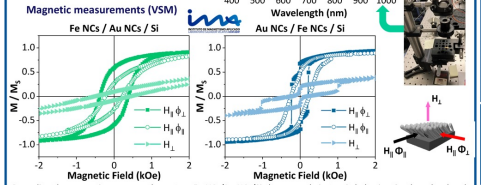
Magnetic and optical characterization: VSM & reflectivity

Optical properties (0° polarization)

Reflectivity measurements demonstrate optical activity in all samples with Au NCs deposited on the top.—Among these, the **vertical NCs** and the bimetallic **Au-NCs/Fe-NCs/Si** system display a **LSPR** peak centered around 500 - 530 nm, being notably more pronounced in the sample containing vertical NCs. The presence of LSPR allows the use of these samples in photothermal treatments.



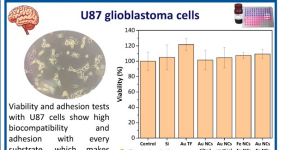
Magnetic measurements (VSM)



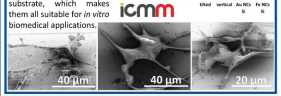
Regarding the magnetic response, the system Fe-NCs/Au-NCs/Si shows nearly isotropic behavior. On the other hand, Au-NCs/Fe-NCs/Si configuration shows different magnetic responses depending on the direction of the applied magnetic field because of a **uniaxial magnetic anisotropy** induced by GLAD growth [4]. The presence of a sharp change (or "jump") in the magnetization curve when the magnetic field is applied perpendicular to the substrate demonstrates the existence of another magnetization easy-axis, which is due to an interface **Au/Fe anisotropy.**

Viability and celular adhesion

U87 glioblastoma cells



Viability and adhesion tests with U87 cells show high biocompatibility and adhesion with every substrate, which makes them all suitable for *in vitro* biomedical applications.



References

1. R. Álvarez et al., *Nanotechnology* **24(4)**, 045604 (2013).
2. A. Espinosa et al., *Advanced Functional Materials* 2018, 28(37).
3. W. Zhang et al., *Physical Chemistry Chemical Physics* 2023, 25(14).
4. E. Navarro et al., Nanomaterials 12(7), 1186 (2022).

Acknowledgements

This work was supported by Ministerio de Ciencia, Innovación y Universidades (FPU grant (M. G.-S.) and projects PID2021-126524NB-100 and PID2021-127033OB-C21), and CSIC (PIE 20226AT024).

FACULTAD DE CIENCIAS FÍSICAS

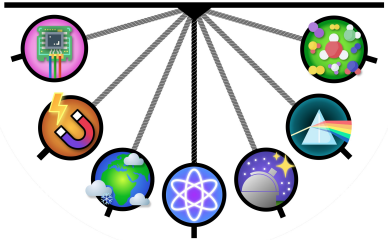
10

Laser-induced sintering of Titanium niobate films from powders of TiO_2 and Nb_2O_5 for energy applications

Gonzalo Gómez Muñoz

ESCUELA DE DOCTORADO
UNIVERSIDAD COMPLUTENSE DE MADRID

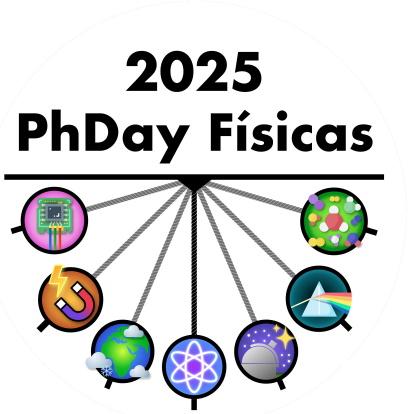
2025 PhDay Físicas



10

Nombre	Gonzalo
Apellidos	Gómez Muñoz
Departamento	FM
Doctorado	Física
Director/es de la Tesis	Belén Sotillo Buzarra y F. Javier Solís Céspedes
Título de la contribución	***Laser-induced sintering of Titanium niobate films from powders of TiO_2 and Nb_2O_5 for energy applications***

2025
PhDay Físicas



Laser-induced sintering of Titanium niobate films from powders of TiO_2 and Nb_2O_5 for energy applications.

G. Gomez-Muñoz[1], A. Calvo-Villoslada[2], I. Álvarez-Serrano[2], M.L. López[2], P. Fernandez[2], J. Solis[1], B. Sotillo[2]

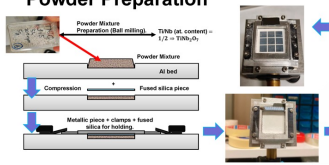
1 Laser Processing Group, Instituto de Óptica "Daza de Valdés" – CSIC, 28006 Madrid, Spain.
2 FIQUI(MAT)[2], Department of Materials Physics – UCM, 28040 Madrid, Spain.

Introduction

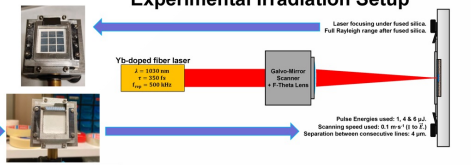
Titanium niobates (TNOs) are a family of materials with diverse stoichiometries and crystalline structures, which turn them into a complex-system that requires highly controlled treatments in order to achieve a proper production. The most stable TNO-structure is $TiNb_2O_7$, which is an oxide that have already proven its excellent performance in emergent applications, specifically for energy storage in Li-ion batteries [1,2].
Recently, the feasibility of inducing the sintering of compact Nb_2O_5 films by fs-laser powder bed fusion while improving their electrical conductivity several orders of magnitude has been demonstrated [3]. For the case of Nb_2O_5, microstructure and anisotropy of the layers were controlled with fs-laser conditions, triggering the stabilisation of a monoclinic oxygen-deficient phase (thus, much more conductive and better for energy storage than stoichiometric niobium oxide). In this work, a similar approach has been followed in order to induce the sintering of compact TNO films starting from a mixture of TiO_2 and Nb_2O_5 powders. A characterization of the sintered films has been performed in order to understand which phases have been induced by fs-laser irradiation of different scenarios depending on how do we change the laser pulse energy.

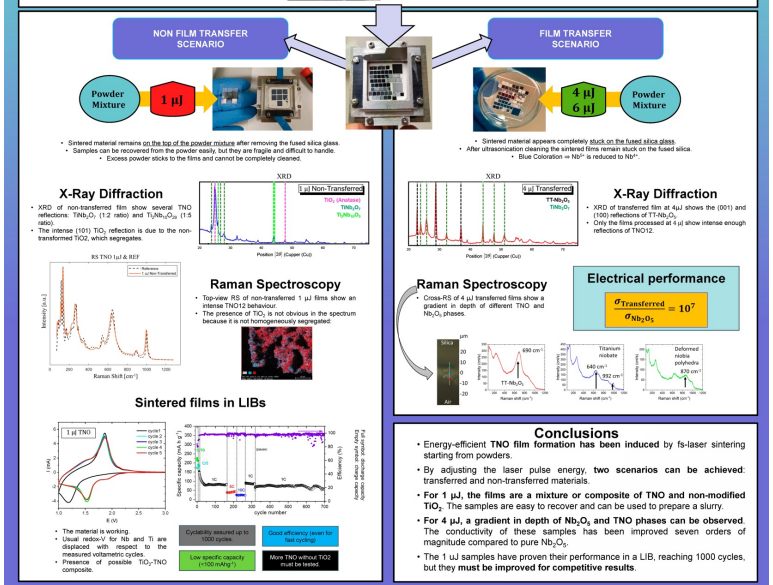
[1] Y. Zhang, et al., *Electrochim. Acta* **330**, 135299 (2020). [2] X. Wu, et al., *Electrochem. Commun.* **25**, 39-42 (2012). [3] B. Sotillo, et al., *Mater. Des.* **224**, 111346 (2022).

Powder Preparation



Experimental Irradiation Setup





Conclusions

- Energy-efficient **TNO film formation has been induced** by fs-laser sintering starting from powders.
- By adjusting the laser pulse energy, **two scenarios can be achieved**: transferred and non-transferred materials.
- **For 1 µJ, the films are a mixture or composite of TNO and non-modified TiO_2**. The samples are easy to recover and can be used to prepare a slurry.
- **For 4 µJ, a gradient in depth of Nb_2O_5 and TNO phases can be observed**. The conductivity of these samples has been improved seven orders of magnitude compared to pure Nb_2O_5.
- The 1 uJ samples have proven their performance in a LIB, reaching 1000 cycles, but they **must be improved for competitive results**.

Acknowledgements

This work has funded by MICIU/AEI/10.13039/501100011033, European Next Generations founds, and Consejería de Educación, Ciencia y Universidades (Comunidad de Madrid) through grants TED2021-130894B-C22, PID2020-112770RB-C21, PID2023-148178OB-C22 and TEC-2024/TEC-85.

FACULTAD DE CIENCIAS FÍSICAS

11

Stability of the Greenland Ice Sheet: from the Last Glacial Maximum to the future

Lucía Gutiérrez González

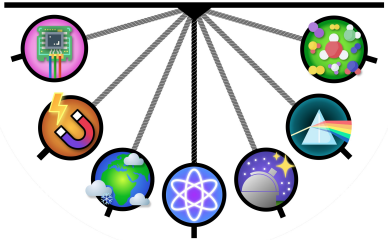
ESCUELA DE DOCTORADO
UNIVERSIDAD COMPLUTENSE DE MADRID

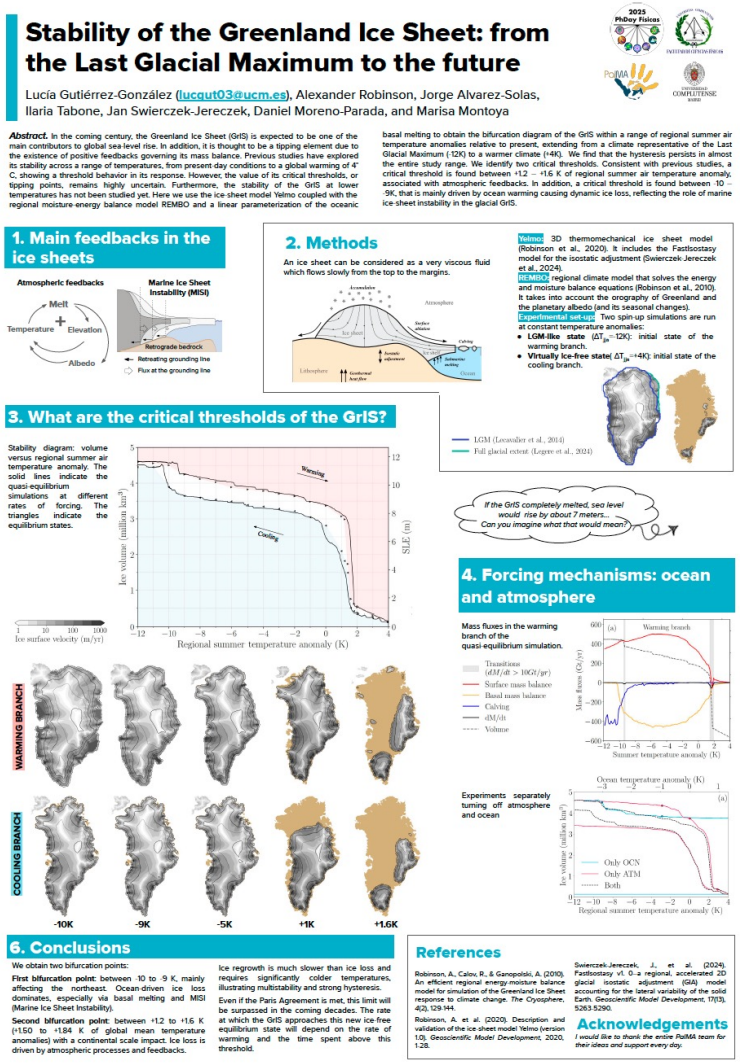
2025 PhDay Físicas

11

Nombre	Lucía
Apellidos	Gutiérrez González
Departamento	FTA
Doctorado	Física
Director/es de la Tesis	María Luisa Montoya Redondo
Título de la contribución	***Stability of the Greenland Ice Sheet: from the Last Glacial Maximum to the future***

2025 PhDay Físicas





FACULTAD DE CIENCIAS FÍSICAS

12

Galaxy clusters through photometric data: from membership to star formation histories

Paula Macías Pardo

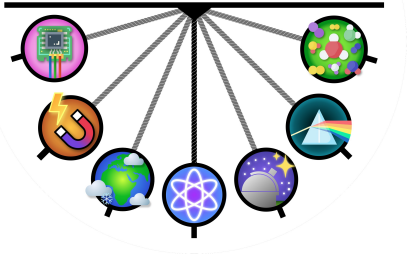
ESCUELA DE DOCTORADO
UNIVERSIDAD COMPLUTENSE DE MADRID

2025 PhDay Físicas

12

Nombre	Paula
Apellidos	Macías Pardo
Departamento	FTA
Doctorado	Astrofísica
Director/es de la Tesis	Armando Gil de Paz y Cristina Catalán Torrecilla
Título de la contribución	***Galaxy clusters through photometric data: from membership to star formation histories***

2025
PhDay Físicas



GALAXY CLUSTERS THROUGH PHOTOMETRY: from membership to star formation histories

Paula Macías Pardo [1,2], Armando Gil de Paz [1,2], Cristina Catalán Torrecilla [1,2], Patricia Sánchez Blázquez [1,2], Jin Koda [3], Masafumi Yagi [4], Hakim Atek [5], CATARSIS team

[1] Departamento de Física de la Tierra y Astrofísica, Universidad Complutense de Madrid, Madrid, España, [2]IPARCOS, Universidad Complutense de Madrid, Madrid, España, [3]Stony Brook University, Stony Brook, NY, USA, [4]National Astronomical Observatory of Japan, Mitaka, Tokyo, Japan, [5] Institut d'Astrophysique de Paris, Paris, France

2025 PhDay Físicas

INTRODUCTION

Galaxy clusters are the most massive bounded systems in the Universe and continue to grow and accrete matter from the cosmic web. Determining the **mass distribution** in galaxy clusters provides essential information about cosmological parameters and the nature of dark matter as they are very sensitive to the underlying cosmological model through quantities such as mass-to-light ratio, X-ray luminosity function, spatial distribution or abundances. It also helps to study the **environmental processes** influencing galaxy evolution [1,2] and the intergalactic medium.

METHODS

X-ray emission	Weak lensing
Jeans equation	Caustic technique

The **caustic technique** [3] takes **positions and velocities** of cluster **members** and projects them into a phase space of cluster-centric distances and radial velocities. The resulting **trumpet-shape** is the result of the increased velocities as galaxies are accelerated by the cluster, and the envelope, the **caustic**, shows the variation of the escape velocity with radius.

CATARSIS

CATARSIS is the new legacy survey for the **3.5m telescope** at the **Calar Alto Observatory**. It will observe a sample of **16 galaxy clusters** at redshifts **z ~ 0.15– 0.23** using the new **TARSIS** instrument (Tetra-ARmed-Super-IFU-Spectrograph), which has an 8 arcmin^2 field of view. The survey will map all objects within the clusters' virial radii, as well as foreground and background galaxies.

Achieving the objectives of the survey requires **precise spectrophotometric calibration**, detailed analysis of disk galaxy spiral morphologies, and measurements of sizes, ellipticities, and position angles. Additionally, the survey aims to **recover very low levels of residual star formation** and compare them with those observed in **cluster periphery** galaxies.

OBJECTIVES

O1 **Getting photometry of CATARSIS clusters well beyond virial radius:**
- Spectro-photometric calibration in the TARSIS wavelength range
- Spectral energy distribution (SED) fitting
- Physical properties of galaxies in clusters (morphology, stellar mass, star formation history...)

O2 **Mass profiles for a subsample of CATARSIS clusters:**
- A2390: Euclid + weak lensing + intra-cluster light
- A2219: Euclid + Sunyaev Zeldovich

O3 **Develop a robust photometric membership criterion :**
- Photometric redshift from SED-fitting + morphological parameters

Abell 2390

One of the CATARSIS clusters is **Abell 2390**, with 2×10^{15} M$\odot$ at **z = 0.228** recently observed in the Euclid ERO [4]. We have used **Euclid** data (**VIS, Y, J, H**), complemented by their pre-imaging deep photometry with **Suprime-Cam**, which provide six band optical coverage (**B, V, Rc, i, Ic, z'**), as well as **CFHT MegaCam u-band** imaging. This dataset has allowed us to derive photometric redshifts within the Euclid field of view through spectral energy distribution fitting using Bagpipes, selecting those compatible with being members of A2390 [6].

INCORPORATING MORPHOLOGY

We take advantage of **deep Subaru/HSC imaging** [9, 10] **for eight nearby clusters** ($z \lesssim 0.05$), which provides high-resolution and high-sensitivity data to **better characterize the galaxies' structural and morphological properties** and integrate them into the membership framework. As part of this work, we are performing a systematic **morphological decomposition with GALFIT** [11] for all detected galaxies in these clusters through **NoiseChisel** [12], measuring structural parameters (e.g. effective radius, Sérsic index, ellipticity) to quantify environmental trends.

UDGs

Recent discovery of a significant population of galaxies with **large effective radii** and **low central surface brightness** mostly in cluster environments: $r_{eff} \geq 1.5$ kpc and $\mu_g \geq 24$ mag/arcsec^2.

Particular attention is being given to **Ultra Diffuse Galaxies (UDGs)** as an extreme population of cluster galaxies. Their detection in the cluster regions, consistent with the expected surface-brightness limits, allows us to **assume cluster membership** and use them as benchmarks to test and calibrate the extended morphological membership framework.

- Answer the question: do UDGs extend the size-luminosity relation as a low-luminosity tail? Or do they form a distinct population? [13]
- This work is being developed in collaboration with international teams, with the goal of producing a public catalog of UDG candidates across the HSC cluster samples

Improve cluster membership

- Need for **spectroscopic** data on **blue, late-type** galaxies beyond the virial radius.
- Explore **scaling relations** [7, 8] and add **morphological information** to better identify blue or late-type members and separate from background galaxies.

Photo-zs are underestimated for *blue members*

WHICH GALAXIES ARE CLUSTER MEMBERS?

REFERENCES

[1] McGaugh, S. et al. 2015, Can. J. Phys., 93, 250
[2] Gladders, M. D. et al. 2007, ApJ, 655, 128
[3] Geller, Margaret J. et al. 2013, ApJ, 764, 58
[4] Atek, H. et al. 2025, A&A, 697, A15
[5] Datta, A. et al. 2024, ApJ, 977, 87
[6] Sola, J. et al. 2020, ApJ, 902, 17
[7] De Propris, R. et al. 2016, MNRAS, 459, 1268
[8] La Barbera, F. et al. 2003, ApJ, 595 127
[9] Komiyama, Y. et al. 2018, PASJ, 70, S2
[10] Aihara, H. et al. 2018, PASJ, 70, S8
[11] Peng, C. Y., Ho, L. C., Impey, C. D., & Rix, H.-W. 2010, AJ, 139, 2097
[12] Akhlaghi, M., & Ichikawa, T. 2015, ApJS, 220, 1
[13] Danieli, S., & van Dokkum, P. 2019, ApJ, 875, L5

ACKNOWLEDGEMENTS:

This research has been funded by the spanish Agencia Estatal de Investigación (AEI) and Ministerio de Ciencia e Innovación (MCIN) under the projects PID2021-126021NB-I00, PID2021-126813NB-C31 and PID2021-123417OB-I00. Authors also acknowledge the financial support from the program Tecnologías Avanzadas para la Exploración del Universo y sus Componentes (TAEC-CM).

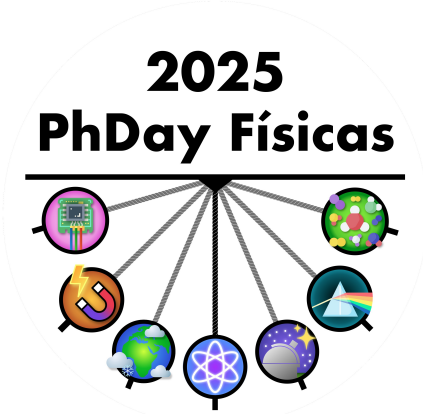
FACULTAD DE CIENCIAS FÍSICAS

13

Performance Assessment of the IEM-CSIC Proton Scanner

Amanda Nathali Nerio Aguirre

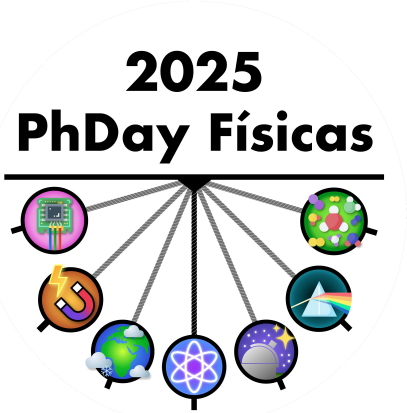
ESCUELA DE DOCTORADO
UNIVERSIDAD COMPLUTENSE DE MADRID



13

Nombre	Amanda Nathali
Apellidos	Nerio Aguirre
Departamento	EMFTEL
Doctorado	Física
Director/es de la Tesis	José Antonio Briz Monago y María José García Borge
Título de la contribución	***Performance Assessment of the IEM-CSIC Proton Scanner***

2025 PhDay Físicas



Performance Assessment of the IEM-CSIC Proton Scanner

Amanda Nerio Aguirre[1], José Antonio Briz[2], María José García Borge[1]

[1] Instituto de Estructura de la Materia, CSIC, Madrid, Spain
[2] Grupo de Física Nuclear (GFN) and IPARCOS, Universidad Complutense de Madrid (UCM), Madrid, Spain

amanda.nerio@csic.es

Proton imaging.
A low-dose imaging technique for proton and hadron therapy that improves:
- **Patient positioning** and **proton range verification**
- **Treatment planning** via direct **relative stopping power (RSP) mapping**

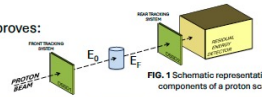


FIG. 1 Schematic representation of the components of a proton scanner.

INTRODUCTION AND MOTIVATION

As proton therapy use is increasing worldwide, **accurate proton range prediction is essential** for the treatment planning. Current treatment planning relies on X-ray imaging to estimate the RSP of tissues.

X-ray imaging	Proton imaging
Indirect RSP estimation	✅ **Direct** RSP measurement
Higher proton range uncertainty [1]	✅ Improved proton **range accuracy**
Higher radiation dose	**Lower** radiation **dose**

Our motivation is to repurpose nuclear detection technologies for medical imaging applications.

Turning research technology into medical innovation

THE SPANISH PROTON SCANNER

- The proton scanner can perform **proton radiography** and **tomography**.
- **Two double-sided silicon strip detectors** (DSSSD) track proton trajectories.
- The **CEPA4 scintillation detector** measures the residual energy of protons.
- It was tested in three campaigns at the Cyclotron Centre Bronowice in Krakow, Poland during 2021 and 2022 [2,3,4].

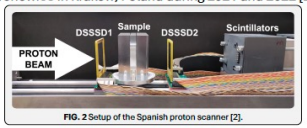
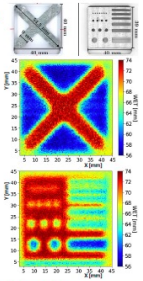


FIG. 2 Setup of the Spanish proton scanner [2].

RESULTS

Proton radiography (pRad)

- Nice pRads were obtained which consistently and reliably reproduced the samples.
- Successfully **distinguished** the different **materials** present.
- Resolved structures as small as **2 mm**.
- Determined the **water equivalent thicknesses** (WET), that represent the radiological thickness of the samples.

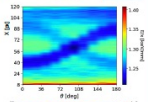


Proton tomography (pCT)

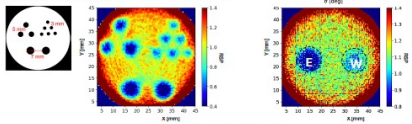
- Tomographic images were obtained using **Filtered Back-Projection** algorithms.
- **RSP** values **in good agreement** with previous works.

Region	RSP [5] I_{mm}	RSP [6] pCT	RSP [4] This work
Water	1.000(4)	1.00(3)	1.000(5)
Ethanol	0.822(3)	0.82(2)	0.829(7)
PMMA	1.168(5)	1.15(3)	1.158(5)





- Resolved structures as small as **3 mm**.



CONCLUSIONS

- pRads and pCT images were obtained using the Spanish proton scanner.
- Spatial resolution **better than 2 mm in pRad** and **better than 3 mm in pCT** with the current prototype.
- **RSP** values **are consistent** with reference values.
- The scanner prototype shows promise for a more accurate RSP mapping while delivering less dose during imaging.

REFERENCES

[1] R. P. Johnson *et al.* Rep. Prog. Phys. **81**, 016701 (2018).
[2] A. N. Nerio *et al.* EPJ Web of Conferences **290**, 08004 (2023).
[3] J. A. Briz *et al.* IEEE Transactions on Nuclear Science, **69** (4), 696-702 (2021).
[4] E. Nácher *et al.* Eur. Phys. J. Plus, **139**, 404 (2024).
[5] J. K. van Abbema *et al.*, NIM B **436**, 99-106 (2018).
[6] A. Terakawa *et al.*, Phys. Med. Biol. **68**, 095023 (2023).

ACKNOWLEDGEMENTS

Work funded by the Comunidad de Madrid (PRONTO-CM, ASAP-CM), the Spanish Ministry of Science (PID2022-140162NB-I00, PID2022-138297NB-C21, PDC2022-133382-I00), and the Generalitat Valenciana (CIPROM/2021/064). Experiments supported by the EU Horizon 2020 programme (ENSAR2 – 654002, INSPIRE – 730983).

FACULTAD DE CIENCIAS FÍSICAS

14

The physics behind Earth's latest ice ages

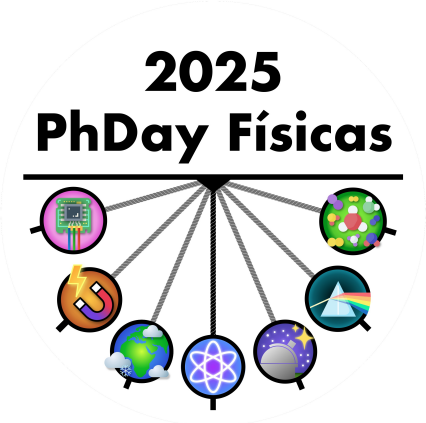
Sergio Pérez Montero

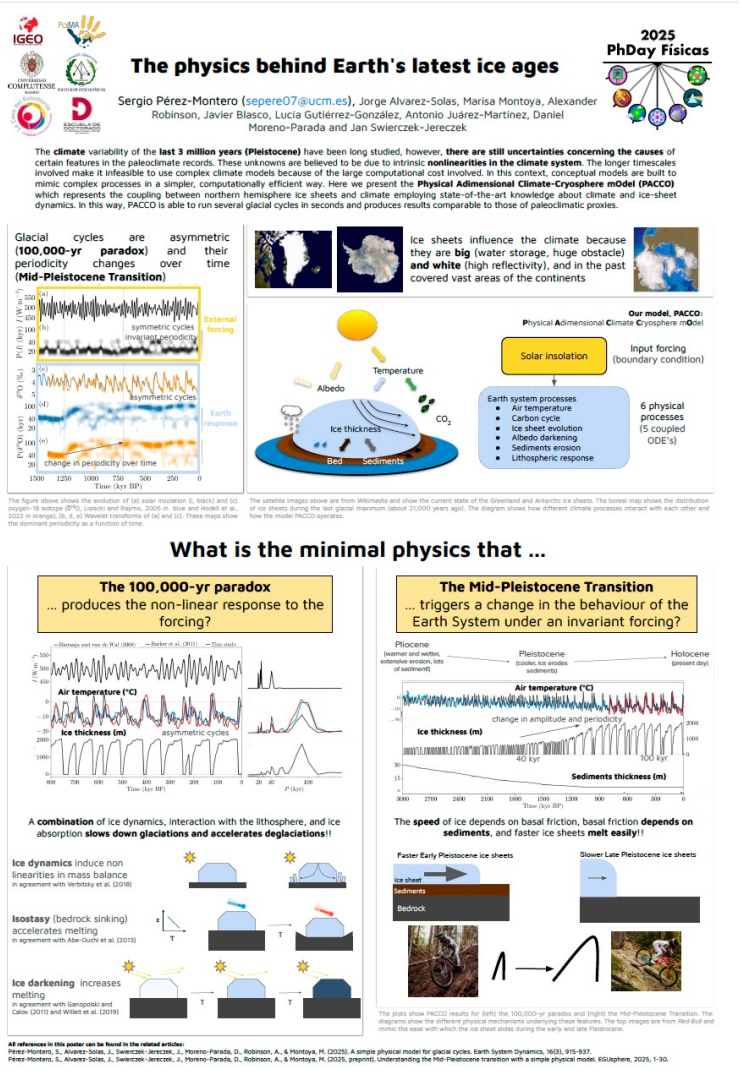
ESCUELA DE DOCTORADO
UNIVERSIDAD COMPLUTENSE DE MADRID

2025 PhDay Físicas

14

Nombre	Sergio
Apellidos	Pérez-Montero
Departamento	FTA
Doctorado	Física
Director/es de la Tesis	Jorge Alvarez-Solas
Título de la contribución	***The physics behind Earth's latest ice ages***





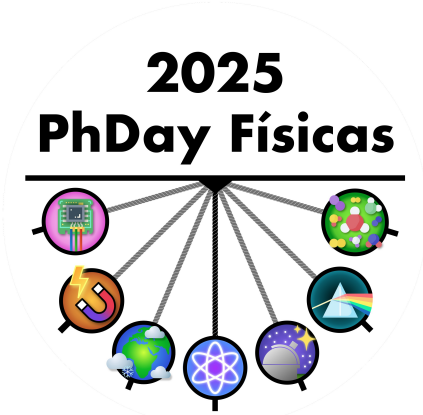
FACULTAD DE CIENCIAS FÍSICAS

15

The first galaxies of the Universe: exploring the Epoch of Reionization with JWST

Carlota Prieto Jiménez

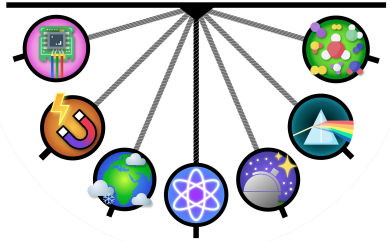
ESCUELA DE DOCTORADO
UNIVERSIDAD COMPLUTENSE DE MADRID

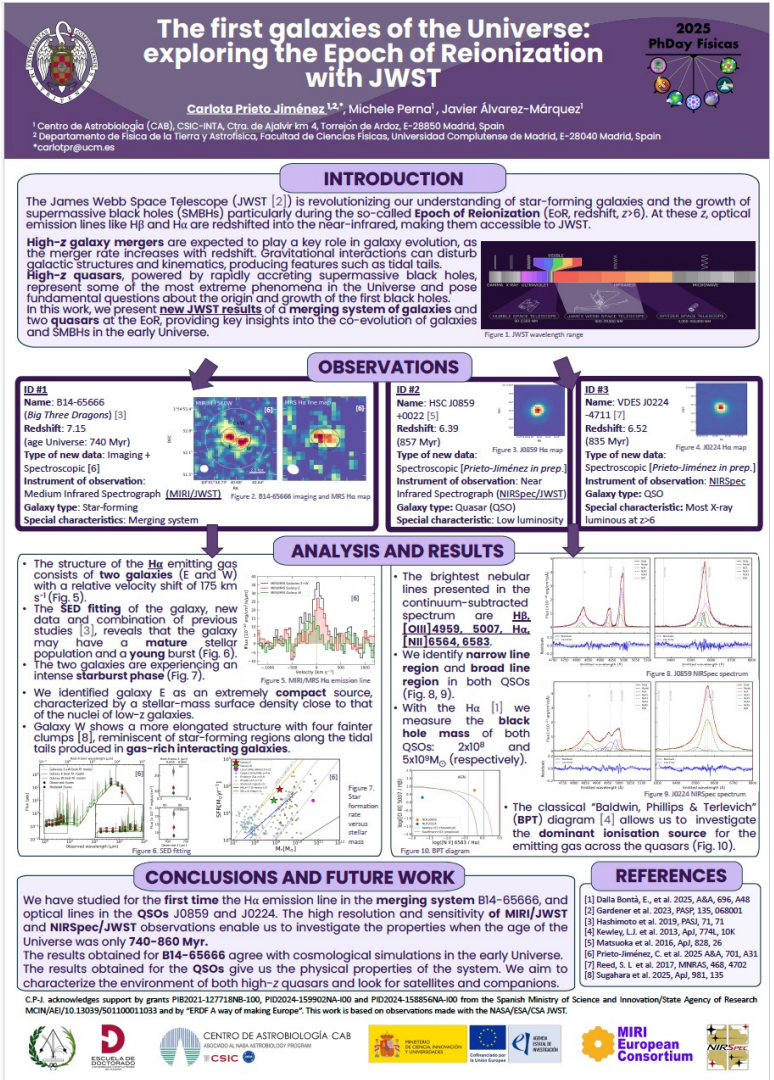


15

Nombre	Carlota
Apellidos	Prieto Jiménez
Departamento	FTA
Doctorado	Astrofísica
Director/es de la Tesis	Javier Álvarez-Márquez y Michele Perna
Título de la contribución	***The first galaxies of the Universe: exploring the Epoch of Reionization with JWST***

2025
PhDay Físicas





FACULTAD DE CIENCIAS FÍSICAS

16

Heat extremes in southern South America: from historical regional analysis to future storylines

Solange Suli Silicaro

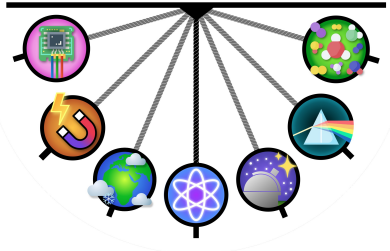
ESCUELA DE DOCTORADO
UNIVERSIDAD COMPLUTENSE DE MADRID

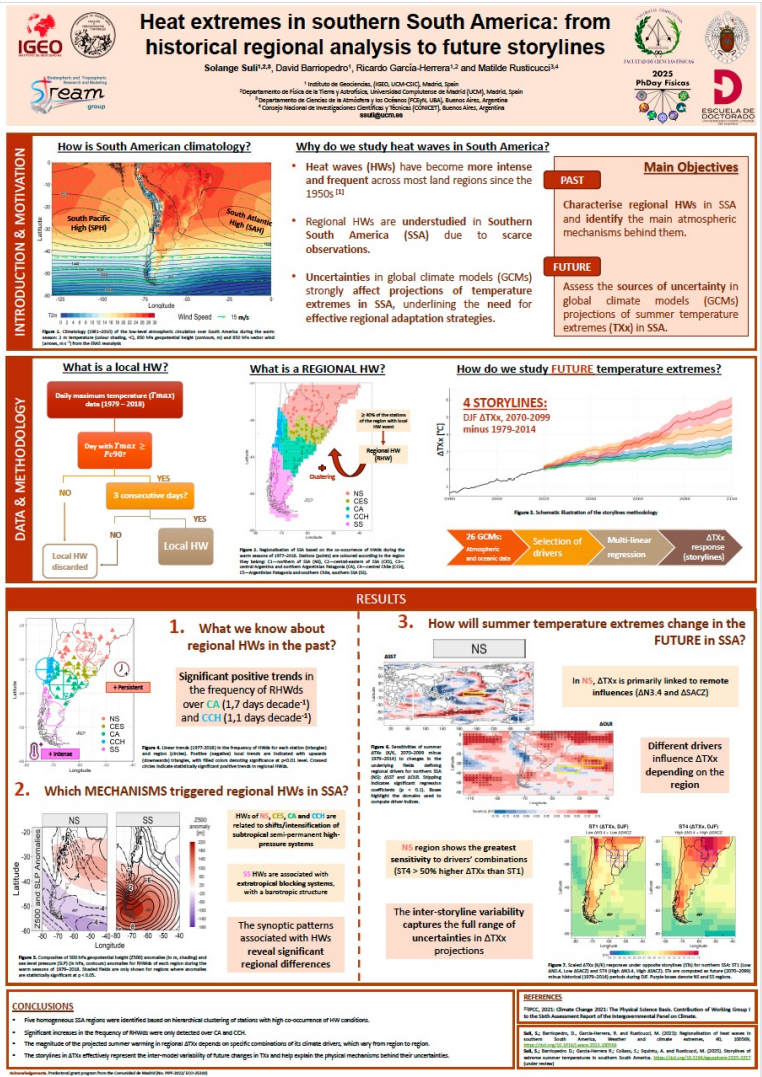
2025 PhDay Físicas

16

Nombre	Solange
Apellidos	Suli Silicaro
Departamento	FTA
Doctorado	Física
Director/es de la Tesis	David Barriopedro Cepero
Título de la contribución	***Heat extremes in southern South America: from historical regional analysis to future storylines***

2025
PhDay Físicas





ESCUELA DE DOCTORADO
UNIVERSIDAD COMPLUTENSE DE MADRID

UNIVERSIDAD COMPLUTENSE MADRID

La Casa del Estudiante
UNIVERSIDAD COMPLUTENSE DE MADRID

2025 PhDay Físicas

